Marine Structures 60 (2018) 72–86

Contents lists available at ScienceDirect

Marine Structures

journal homepage: www.elsevier.com/locate/marstruc

A novel framework for deriving the unified SCF in multi-planar overlapped tubular joints

Jian Zhang[a,*], Jin Jiang[b,**], Wei Shen[c,***], Ying Luo[a]

[a] National Center for International Research on Structural Health Management of Critical Components, Institute of Structural Health Management, Department of Mechanics and Engineering Science, Jiangsu University, Zhenjiang 212013, PR China

[b] School of Civil Engineering, Guangzhou University, Guangzhou 510006, PR China

[c] Centre for Offshore Research and Engineering, Department of Civil and Environmental Engineering, National University of Singapore, 1 Engineering Drive 2, 117576, Singapore

ARTICLE INFO

Keywords:
Stress Concentration Factor (SCF)
Hot spot stress method
Fatigue
Multi-planar overlapped
Tubular joint
KK-joint
Jack-up

ABSTRACT

For the past few decades, a significant number of research efforts have been devoted to the studies of SCF values and parametric design formulae at certain positions in various uniplanar and multi-planar tubular joints. However, very few investigations on the multi-planar overlapped tubular joints have been reported. The main reason may lie in the complexity of combining effects between multi-planarity and overlapping. In this paper, a novel framework for deriving the unified SCFs is proposed by reducing joint modeling from multi-planar out-of-plane overlapping to equivalent uniplanar non-overlapping. By integrating the equivalent beam model with solid finite element modeling for the overlapped tubular *KK*-joint in offshore jack-ups, the procedures for computing the unified SCF values in the equivalent beam stick model are successfully developed. Verification of the proposed framework is obtained by comparing the unified SCFs based on basic load cases with those based on actual wave loading typically experienced by the jack-up.

1. Introduction

Circular hollow section (CHS) members are widely used as the primary components in offshore tubular lattice structures such as jack-ups [1]. The circular hollow sections are joined together to form a tubular joint where the profiled ends of secondary members (the braces) are welded onto the circumference of the main member (the chord). Due to the complex geometry of such joints, cyclic wave loading on offshore structures may induce localized fatigue damage and failure as a result of high stress concentration at the vicinity of brace-to-chord intersections. For the purpose of fatigue design, the hot spot stress method [2] has been quite efficient and widely used to predict the fatigue life of offshore tubular joints. In this method, the nominal stress range at the joint members is multiplied by an appropriate stress concentration factor (SCF) to provide the geometric stress at a certain location. The SCF is the ratio of the local surface stress at the brace-to-chord intersection to the nominal stress in the brace [3]. Geometric stresses are calculated at various locations around the welded region and the maximum geometric stress is the hot spot stress (HSS). The fatigue life of the joint is estimated through an appropriate *S-N* fatigue curve [2], *N* being the number of load cycles. Therefore, the hot spot stress method depends on the accurate prediction of SCFs for tubular joints.

* Corresponding author.
** Corresponding author.
*** Corresponding author.
E-mail addresses: jianzhang@ujs.edu.cn (J. Zhang), jiangjin@gzhu.edu.cn (J. Jiang), ceesw@nus.edu.sg (W. Shen).

https://doi.org/10.1016/j.marstruc.2018.03.008
Received 31 July 2017; Received in revised form 27 February 2018; Accepted 19 March 2018
0951-8339/

A significant number of research programs have been carried out over the past thirty years on the study of parametric design formulae and SCF values at certain positions in various uniplanar tubular joints, in which the axes of the chord member and brace members reside in the same plane [4–12]. If the axes of the brace members, as well as the chord member, are in different planes, they are considered as multi-planar joints. Multi-planar joints dominate the practical applications for offshore tubular structures, which are generally three-dimensional truss structures. Multi-planarity effects play an important role in the stress distribution at the vicinity of joint intersection. Thus, the parametric formulae of uniplanar tubular joints for SCF prediction may not be suitable for such multi-planar connections. In the context of research effort on multi-planar joints, much fewer investigations have been reported due to the complexity and high cost involved. Karamanos et al. [13] and Chiew et al. [14] developed parametric equations to determine the SCFs for multi-planar tubular XX-joints. Karamanos et al. [15,16] proposed SCF equations in multi-planar tubular DT-joints including axial and bending effects. Van Wingerde et al. [17] presented simplified SCF formulae and graphs for multi-planar KK-connections, while Woghiren and Brennan [18] proposed a set of parametric SCF equations for multi-planar stiffened tubular KK-joints. Lotfollahi-Yaghin and Ahmadi [19] and Ahmadi and Zavvar [20] performed parametric SCF studies for multi-planar KT-joints under axial, in-plane and out-of-plane bending loads.

Due to the ease of fabrication and the availability of many assessment methods for ultimate strength and fatigue performance, non-overlapped joints [4,6,10,17–20] are widely used for the construction of many tubular structures. However, when the brace-to-chord diameter ratio is higher than 0.7, non-overlapped *K*-joints may not be easily designed due to the limited validity range of design code [21]. Instead, an overlapped joint may be needed, which can be in-plane (the chord axis rests in the same plane with the axes of overlapped braces) or out-of-plane (the chord axis rest in a different plane from the axes of overlapped braces). By partially overlapping the brace, the chord eccentricity and unbalanced moment due to the gap between the braces could be eliminated [22]. In general, an overlapped CHS *K*-joint has a higher fabrication cost than a non-overlapped *K*-joint due to the more complex intersection profile and construction procedure. However, an overlapped CHS *K*-joint outperforms its non-overlapped counterpart in terms of ultimate strength capacity [23], cost effectiveness [24] and fatigue strength [25]. Efthymiou and Durkin [4] developed the SCF and HSS equations for partially overlapped joints based on a small scale finite element study involving 100 joint configurations and loading cases. Their equations were verified experimentally by Dharmavasan and Seneviratne [26] using scaled down acrylic models and it was found that overlapping helps reduce the chord SCFs. Lee et al. [22] carried out full scale tests on overlapped CHS *K*-joints and found that the formulae of Ethymiou and Durkin [4] are conservative only when the joints were subjected to in-plane bending loading, but not for the case of axial loading. Lee et al. [27] conducted a parametric numerical study to compare the fatigue performances of non-overlapped and partially overlapped CHS *K*-joint under different loading conditions. They concluded that, as during actual truss design most of the members will be assumed to be axially loading only, a partially overlapped CHS *K*-joint could be regarded as a favorite when comparing with its non-overlapped counterpart in terms of fatigue performance. Research on fatigue behavior of overlapped tubular *K*-joints with an overlapping ratio, the overlapped length to the diameter of the brace, larger than 50% can be found in the works of Gao et al. [8], Gho et al. [28] and Pang et al. [29].

The research efforts expanded so far on the overlapped tubular joints are mainly for uniplanar *K*-joint with in-plane overlapping. However, very few investigations on the multi-planar overlapped tubular joints, which indicate that the axis of the chord member resides in a different plane from the axes of overlapped brace members, have been reported. One of the main challenges is possibly that multi-planar overlapped joint normally involves out-of-plane overlapping. Another challenge may lie in the complexity of combining effects between multi-planarity and brace overlapping.

To address the above challenges, a general framework for deriving the unified SCFs in multi-planar overlapped tubular joints is proposed in this paper. Taking the multi-planar overlapped tubular *KK*-joint in offshore jack-ups as an example, an equivalent beam stick model is firstly proposed to simplify modeling procedure for the joint. Then, a calculation procedure for the unified SCFs is devised based on basic loading cases using the solid joint model and its equivalent beam model. The calculation procedure is further developed for the SCFs based on actual wave load cases experienced by the jack-up. Verification of the proposed framework is subsequently obtained by comparing the unified SCFs based on basic load cases with those obtained by actual wave loading. Lastly, conclusions from the present study are given.

2. Multi-planar overlapped joint modeling

2.1. Background

Jack-up is a mobile self-elevating drilling unit used for offshore oil and gas exploration in shallow water. It typically comprises a buoyant, approximately triangular hull supported by three lattice legs, each resting on a large inverted conical footing (spudcan). The multi-planar overlapped *KK*-joint under investigation is an integral part of the lattice legs, as shown in Fig. 1. The schematic diagram of a multi-planar overlapped *KK*-joint is plotted in Fig. 2. It can be observed that the axes of the chord and the overlapping braces are in different planes.

For fatigue design of non-overlapped tubular joints, the hot spot stress is calculated as the nominal stress in a brace multiplied by appropriate SCFs [3]. Carry-over effect is defined as the stress concentration at a certain location near the weld toe due to a load (axial or bending) on another brace. Refer to the joint of Fig. 2, the local stress at a weld location of brace (a) or brace (b) due to a load on brace (c) is a "carry-over effect". In such a case, braces (a) and (b) are called the "reference brace", while brace (c) is the "carry-over brace". According to the studies by Karamanos et al. [15,16] for multi-planar non-overlapped tubular joints, stress concentrations due to carry-over effects can be neglected at crown locations of the reference brace for both axial and bending cases. However, due to overlapping effects, stress concentrations should be considered at crown locations of the overlapping (reference)

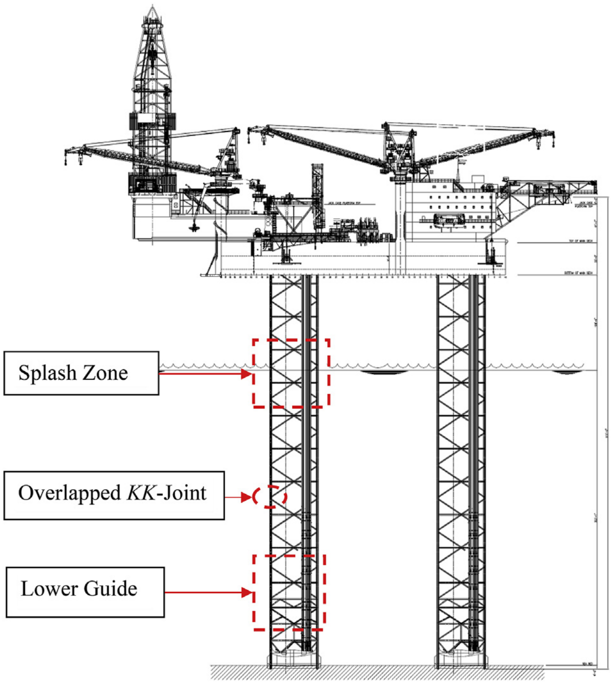

Fig. 1. Side view of a jack-up with multi-planar overlapped *KK*-joints.

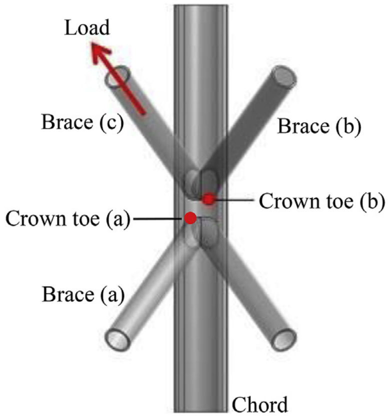

Fig. 2. Schematic diagram of a multi-planar overlapped *KK*-joint.

brace, for example the crown toe (b) as shown in Fig. 2.

2.2. Finite element modeling

Hot spot stress of the tubular joints is obtained by multiplying the nominal stresses with the SCFs. Since no parametric SCF equations are available for multi-planar overlapped tubular joints, the SCF values are often determined for a selection of critical joints using finite element (FE) analysis. A detailed FE joint model with 20-node solid (brick) elements was analyzed in ANSYS [30] with unit pressure and moment applied on the brace end for axial and bending cases, respectively. Fig. 3 presents stress contour for a critical overlapped *KK*-joint under axial loading case with unit pressure on the carry-over brace. The component stresses near the joint location are then extrapolated to the weld toe and converted to principal stresses to determine the SCF. Details on the stress extrapolation can be referred to DNVGL-RP-C203 [2].

It should be stressed that the numerical determination of SCF depends on weld profile, boundary conditions, element type, mesh refinement, integration scheme, extrapolation method, and type of stress used for SCF calculation. Hence, from the viewpoint of fatigue design, there could be some uncertainties due to the use of SCFs obtained from the FE analysis. To this end, a general framework for deriving the unified SCFs by accounting for fatigue design and fatigue damage is needed in practical applications.

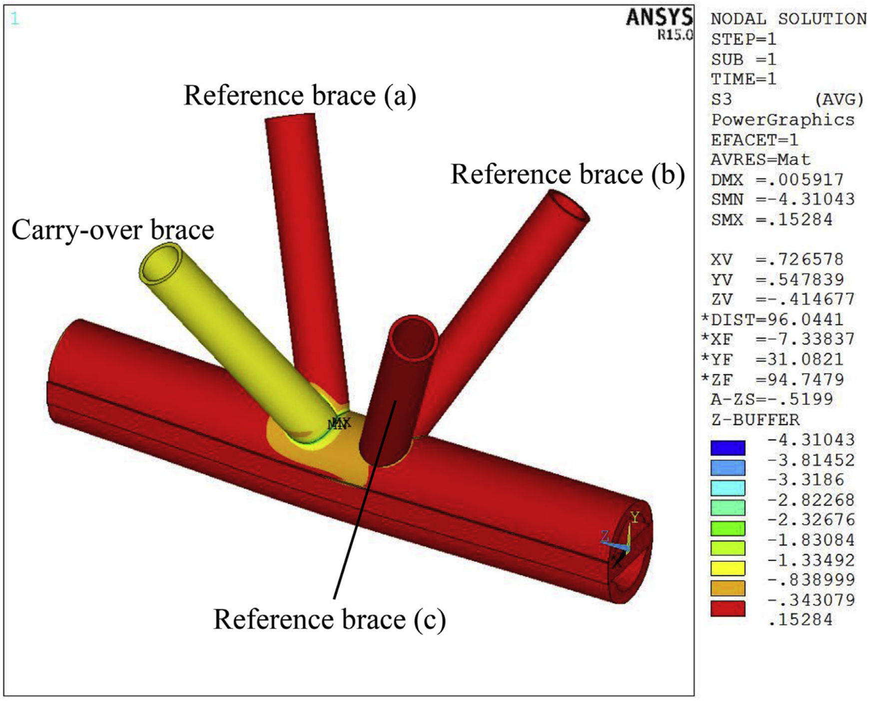

(a)

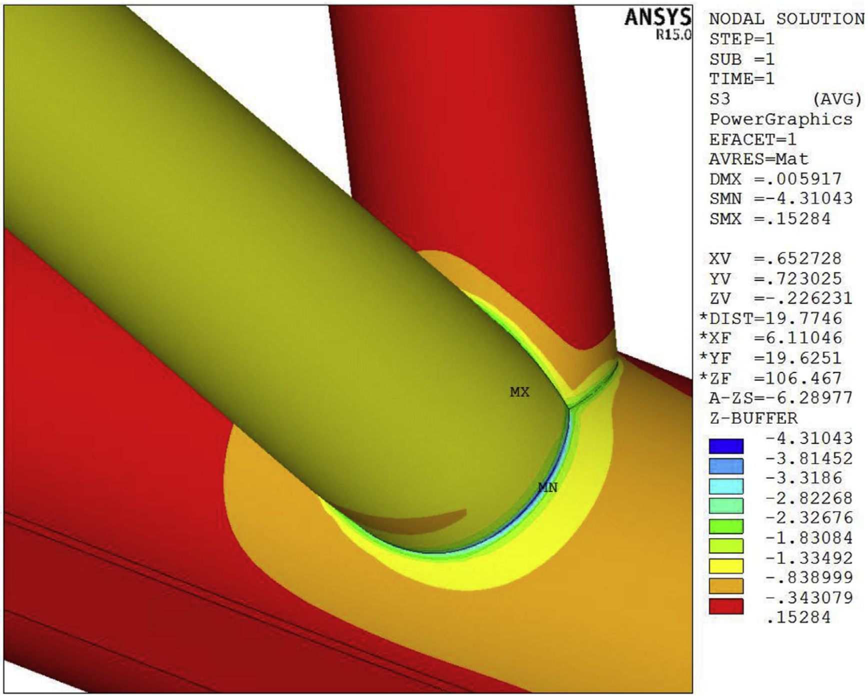

(b)

Fig. 3. Stress contour for a critical overlapped *KK*-joint under axial loading: (a) a full view of the model and (b) a close view of the loading (carry-over) brace and the overlapping (reference) brace.

2.3. Fatigue damage evaluation

For practical applications, the result of a fatigue analysis is usually presented in terms of accumulated damage or fatigue life. It is assumed that the long term distribution of stresses is represented by a two-parameter Weibull distribution [2,3]:

$$Q(\Delta\sigma) = \exp\left[-\left(\frac{\Delta\sigma}{q}\right)^h\right] \tag{1}$$

where Q is the probability for exceedance of the stress range $\Delta\sigma$, h and q are Weibull parameters. The accumulated fatigue damage is then given by

$$D = \frac{N_0}{\bar{a}} q^m \Gamma\left(\frac{m}{h} + 1\right) \tag{2}$$

where Γ is the gamma function, N_0 is the number of cycles in the period under consideration, $\bar{a}$ are coefficients, m is the inverse slope of the *S-N* curve. The Weibull parameter q may be related to the stress range $\Delta\sigma_0$ as follows

$$q = \frac{\Delta\sigma_0}{(\ln N_0)^{1/h}} \tag{3}$$

Since N_0, $\bar{a}$, h and m are constant, fatigue damage can be expresses as

$$D \propto (\Delta\sigma_0)^m \tag{4}$$

Based on the industrial guidelines (Section 2.4.6 in DNVGL-RP-C203 [2] and Section 7.8 in DNVGL-RP-C104 [3]), $m = 3$ is recommended for *S-N* curves of tubular joints in air ($N \le 10^7$ cycles), seawater with cathodic protection ($N \le 1.8 \times 10^6$ cycles) and seawater free corrosion, and $m = 5$ for tubular joints in air ($N > 10^7$cycles) and seawater with cathodic protection ($N > 1.8 \times 10^6$ cycles). Therefore, fatigue damage is proportional to $(\Delta\sigma_0)^m$. Accordingly, fatigue damage is proportional to $(SCF)^m$.

2.4. An equivalent model for the overlapped joint

Carry-over effect can be observed from Fig. 3(a) for braces (a), (b) and (c). However, the local stresses at the weld toe of braces (b) and (c) are negligible compared to those at the weld toe of brace (a). This is obviously due to the overlapping effect between the carry-over brace and the brace (a), as found from a close view of these two braces in Fig. 3(b).

Inspired by the above phenomenon, an equivalent beam stick model for the multi-planar overlapped *KK*-joint is proposed as in Fig. 4. A short beam is adopted to model the overlapped part between the carry-over and reference braces. In this study, the length of short beam is taken as 1 ft and its properties are assumed as the same with the braces. The loading of short beam depends on the combining effects of the carry-over and reference braces. Therefore, it is considered that the short beam is able to capture not only the carry-over effect but also the overlapping effect at the overlapped joint.

3. A general framework for deriving the unified SCFs

The proposed framework is to derive the unified SCFs for the short beam in the equivalent beam stick model of the jack-up. Here "unified" means that in the context of jack-up fatigue design, the unified SCFs would provide equivalent fatigue damage for the actual loading cases, although they are obtained from basic load cases. That is, for a jack-up under a wave loading case, the unified SCFs might not give correct fatigue damage for each individual wave direction; nevertheless, the total fatigue damage of all wave directions can match well with the actual fatigue damage. In this regard, calculation of the short beam SCFs from a general sense excludes the need of calculating for each actual case, or for the same type of joints at different locations. The detailed procedures will be elaborated as below.

3.1. The unified SCFs based on basic load cases

The fatigue life of tubular joints is mainly governed by significant axial loadings in the jack-up. According to the definition in Section 2.1, the intersection of chord and one brace in the reference plane, i.e. brace (b) in Fig. 2, is selected for derivation of the unified SCFs. The axial load cases for the multi-planar overlapped *KK*-joint are presented schematically in Table 1. Although "over-

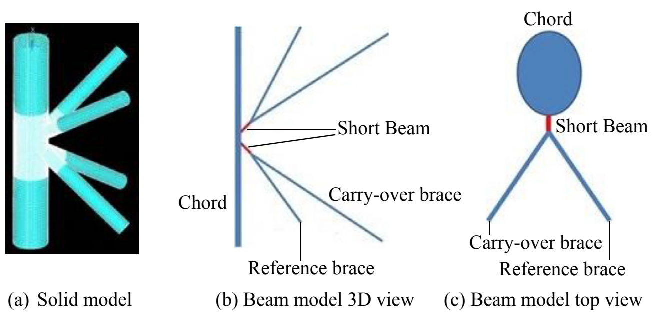

Fig. 4. The solid model and its equivalent beam model. for the multi-planar overlapped *KK*-joint.

Table 1
Schematic diagrams of basic load cases for the multi-planar overlapped KK-joint.

Load case	Balanced	Unbalanced	Over-balanced
	1	1-u	1-o
Reference plane	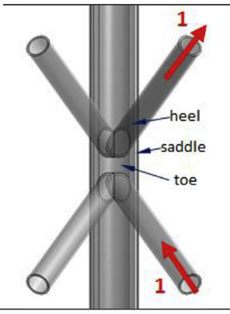	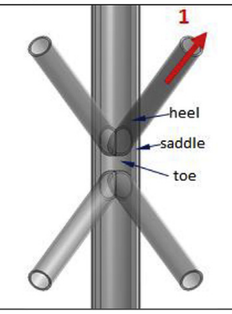	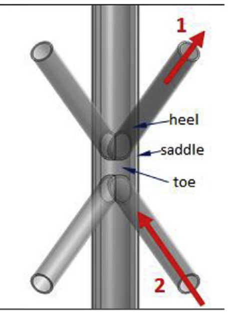
	2	2-u	2-o
Carry-over plane	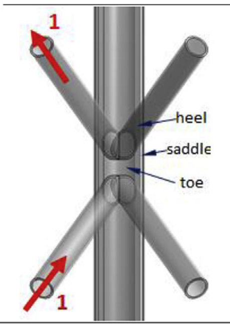	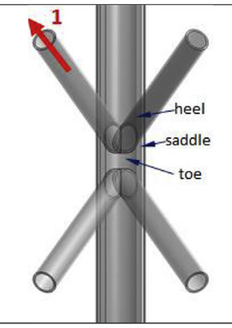	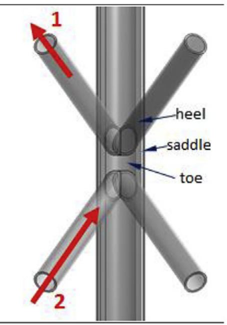
	3	3-u	3-o
Multi-plane	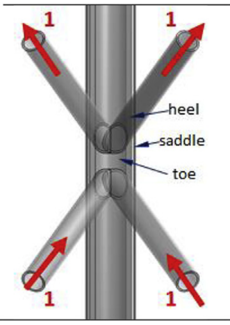	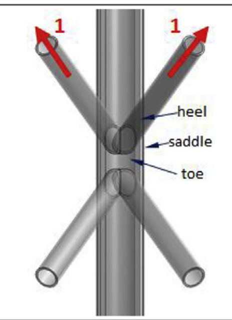	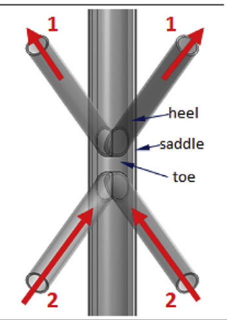

balanced" can be generally categorized as "unbalanced", over-balanced loading will have different effects from the unbalanced loading on the SCFs at the intersection of chord and the selected reference brace. Therefore, with reference to the selected reference brace, basic load cases are denoted at the reference plane, carry-over plane and multi-plane for balanced, unbalanced and over-balanced loadings, respectively. Following the structural design of jack-up truss leg, it is expected that balanced loadings are most common for the out-of-plane overlapped joints. Therefore, only basic balanced load cases with unit loading of 1 ksi on each brace are selected from the axial load cases for the unified SCF calculation (in the following sections, "basic load cases" means basic balanced load cases if not stated otherwise). Fig. 5 shows the schematic (top) view of basic load cases for joint A at various shear directions of jack-up leg. Basic load case 1 corresponds to jack-up leg shear directions of 120 and 300°. Basic load case 2 is related to leg shear directions of 0 and 180°, and basic load case 3 for leg shear directions of 60 and 240°. Probability for different basic load cases can be applied. Here for convenience, it is assumed that all basic load cases have the same probability.

The calculation procedure for the unified SCF based on basic joint load cases is illustrated in Fig. 6, which includes the following steps:

(1) For each basic load case *i*, hot spot stress $\sigma_{bhot(i)}$ is computed based on the FE analysis of solid overlapped joint model. The detailed procedure can be found in Section 2.2;
(2) For each basic load case *i*, short beam nominal stress $\sigma_{bnom(i)}$ is extracted from the equivalent beam joint model;
(3) The equivalent SCF, $SCF_{equ(i)}$ for each load case *i* is then obtained from the hot spot stress divided by short beam nominal stress:

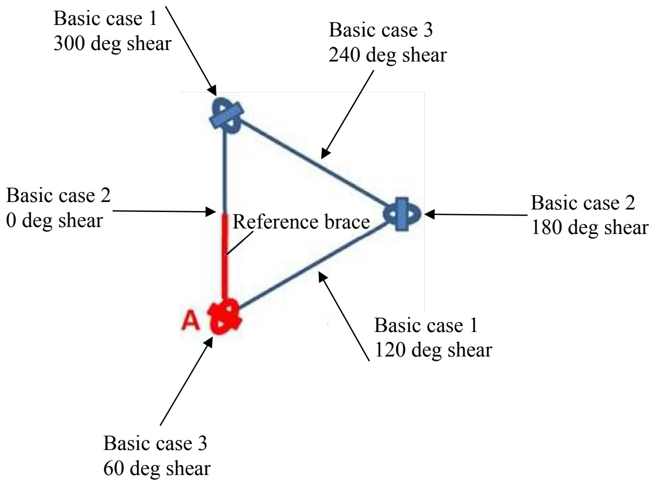

Fig. 5. Schematic view of basic load cases for joint A at various leg shear directions.

$$SCF_{equ\,(i)} = \sigma_{bhot\,(i)}/\sigma_{bnom\,(i)} \tag{5}$$

(4) The unified SCF, SCF_{uni} is proposed and taken as the following form of equivalent SCFs for basic load cases:

$$SCF_{uni} = \left(\sum_{i=1}^{n} (SCF_{equ\,(i)})^m/n\right)^{1/m} \tag{6}$$

where n is the number of basic load cases and n is equal to 3 in this circumstance, m is taken as the inverse slope of the corresponding *S-N* curve. Two assumptions are applied here. Firstly, identical probability is assumed for each basic load case, i.e., wave loading from different leg shear directions between 0 and 300° as shown in Fig. 5 has equal probability. Secondly, as described in Section 2.3, it is assumed that fatigue damage is proportional to $(SCF)^m$, where m is equal to 3 or 5. Here for convenience, $m = 3$ is adopted in the following procedures and calculations. The effects of using $m = 5$ will be discussed later in Section 3.2.

Following the above procedure, the equivalent SCFs for basic load cases are listed in Table 2, and the unified SCF for short beam in Table 3. It is found that the unified SCF for short beam has larger values at the locations of toe, heel and saddle on the brace side than those on the chord side. This demonstrates the similar phenomenon with the uniplanar non-overlapped *K*-joint subject to axial brace loading. In other words, the proposed short beam model reduces joint SCF modeling from multi-planar overlapped *KK*-joint to equivalent uniplanar non-overlapped *K*-joint. The unified SCF values for short beam in the equivalent beam stick model will be validated based on actual wave loading experienced by the jack-up in the following section.

The equivalent SCFs for basic cases with unbalanced and over-balanced loadings are listed in Table 4 and Table 5, respectively.

3.2. Verification of the unified SCFs by actual wave loading

The unified SCFs proposed in the above section based on basic load cases should give the equivalent fatigue damage for the overlapped joint when used for actual wave loading cases experienced by the jack-up. In this section, the unified SCFs are firstly derived based on actual wave loading cases. Subsequently, the obtained SCF values are compared with the unified SCFs based on basic loading cases as derived in Section 3.1.

A typical wave scatter diagram in the North Sea is used. A representative wave in the most probable zone of the scatter diagram is selected with significant wave height of 10.68 ft and zero-crossing period of 7.39 s. As illustrated in Fig. 7, a global jack-up beam stick model under hull-elevated condition is assessed. Wave loading is applied from 0 to 330° in the interval of 30° with a total of 12 wave load directions.

Fig. 7 shows how the unified SCF is calculated based on the actual wave load cases. The procedure is elaborated as follows:

(1) For each wave load direction *i,* brace loadings are extracted from the global jack-up model for the selected overlapped joint;
(2) Apply the extracted brace loadings to the solid joint model to get the actual hot spot stress $\sigma_{ahot(i)}$;
(3) Apply the extracted brace loadings to the equivalent joint stick model to get the nominal stress $\sigma_{anom(i)}$ for the short beam;
(4) Assign an initial unified SCF, SCF_{uni} for the short beam, and the equivalent hot spot stress for the selected joint under wave direction i is calculated as

$$\sigma_{ehot\,(i)} = \sigma_{anom\,(i)}\, SCF_{uni} \tag{7}$$

(5) As described in Section 2.3 and Section 3.1, the joint fatigue damage is assumed to be proportional to (*hot spot stress range*)^m.

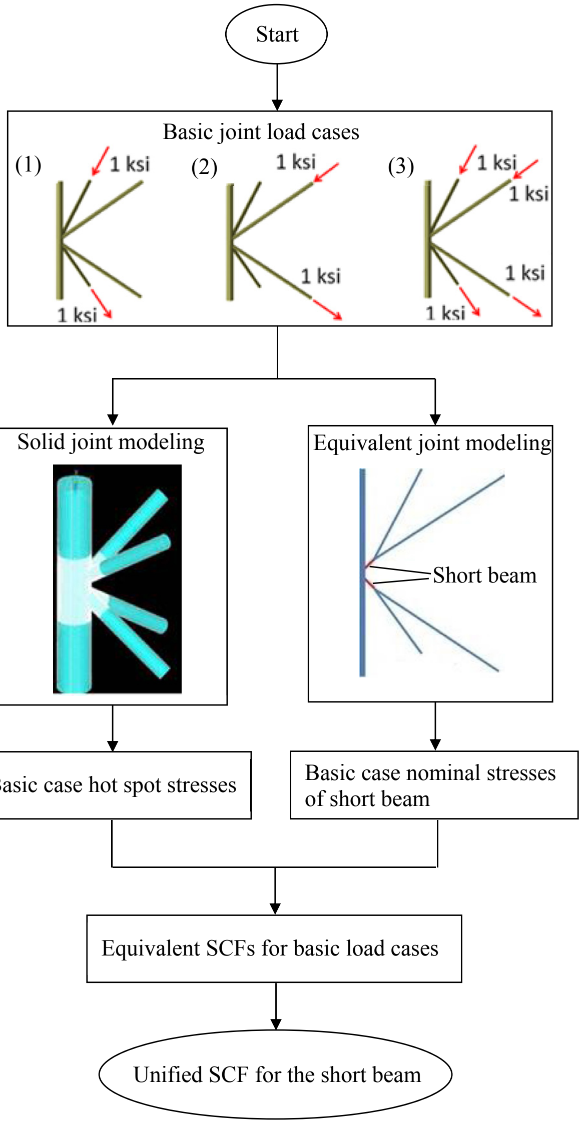

Fig. 6. Calculation procedure for the unified SCF based on basic joint load cases.

Table 2
Calculation of equivalent SCFs for basic load cases.

Load case (i)		1	2	3
		Reference plane	Carry-over plane	Multi-plane
$\sigma_{bhot(i)}$	Chord @ Toe	0.644	0.541	1.052
	Brace @ Toe	1.449	1.326	2.587
	Chord @ Heel	0.185	0.084	0.263
	Brace @ Heel	1.198	0.162	1.124
	Chord @ Saddle	0.586	0.282	0.510
	Brace @ Saddle	1.099	0.250	0.918
$\sigma_{bnor(i)}$		0.910	0.910	1.820
$SCF_{equ(i)}$	Chord @ Toe	0.707	0.595	0.578
	Brace @ Toe	1.593	1.457	1.422
	Chord @ Heel	0.203	0.092	0.145
	Brace @ Heel	1.316	0.178	0.617
	Chord @ Saddle	0.644	0.310	0.280
	Brace @ Saddle	1.208	0.275	0.504

Table 3
The unified SCF for short beam calculated based on basic load cases.

Location	Unified SCF
Chord @ Toe	0.632
Brace @ Toe	1.494
Chord @ Heel	0.159
Brace @ Heel	0.944
Chord @ Saddle	0.474
Brace @ Saddle	0.861

Table 4
Calculation of equivalent SCFs for unbalanced load cases.

Load case (i)		1-u	2-u	3-u
		Reference plane	Carry-over plane	Multi-plane
$\sigma_{bhot(i)}$	Chord @ Toe	1.134	0.790	1.870
	Brace @ Toe	1.529	1.387	2.724
	Chord @ Heel	0.233	0.319	0.417
	Brace @ Heel	1.251	0.258	1.242
	Chord @ Saddle	0.743	0.226	0.612
	Brace @ Saddle	1.252	0.252	1.074
$\sigma_{bnom(i)}$		0.910	0.910	1.820
$SCF_{equ(i)}$	Chord @ Toe	1.246	0.868	1.028
	Brace @ Toe	1.681	1.524	1.497
	Chord @ Heel	0.256	0.351	0.229
	Brace @ Heel	1.374	0.284	0.683
	Chord @ Saddle	0.816	0.248	0.336
	Brace @ Saddle	1.376	0.277	0.590

Table 5
Calculation of equivalent SCFs for over-balanced load cases.

Load case (i)		1-o	2-o	3-o
		Reference plane	Carry-over plane	Multi-plane
$\sigma_{bhot(i)}$	Chord @ Toe	0.179	0.403	0.492
	Brace @ Toe	1.370	1.268	2.435
	Chord @ Heel	0.518	0.240	0.754
	Brace @ Heel	1.135	0.211	0.983
	Chord @ Saddle	0.541	0.431	0.556
	Brace @ Saddle	0.958	0.308	0.780
$\sigma_{bnom(i)}$		0.910	0.910	1.820
$SCF_{equ(i)}$	Chord @ Toe	0.197	0.443	0.270
	Brace @ Toe	1.505	1.393	1.338
	Chord @ Heel	0.569	0.264	0.414
	Brace @ Heel	1.247	0.232	0.540
	Chord @ Saddle	0.595	0.474	0.305
	Brace @ Saddle	1.053	0.338	0.429

Define *(hot spot stress range)*^{m} ($m = 3$) as a fatigue damage factor S, based on actual hot spot stress it has

$$S_a = \sum_{i=0deg}^{330deg} (\sigma_{ahot\,(i)})^3 \tag{8}$$

And from equivalent hot spot stress it has

$$S_e = \sum_{i=0deg}^{330deg} (\sigma_{ehot(i)})^3 \tag{9}$$

Fatigue damages in equations (8) and (9) are summation of damages from all wave load directions. Probability for each wave load direction can be applied. Here for convenience, it is assumed that all wave directions have the identical probability.

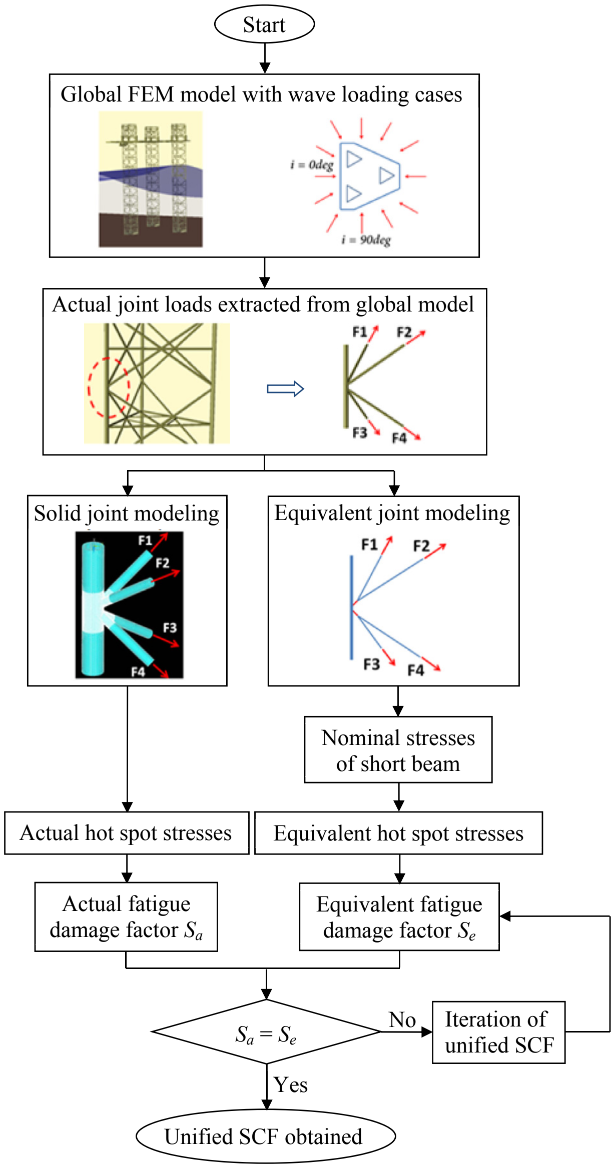

Fig. 7. Calculation procedure for the unified SCF based on actual wave loading.

(6) Compare the values of S_a and S_e. If S_e is bigger than S_a adjust SCF_{uni} to a lower value, and vice versa. Do iteration for Step 4 and Step 5. When S_e equals S_a, the unified SCF is finalized.

Detailed calculation results of the unified SCFs at various brace-to-chord intersections for the selected joint at the splash zone of jack-up leg (see Fig. 1) are listed in Table 6. To better illustrate the iteration process for determining the value of SCF_{uni}, a more detailed calculation procedure for the intersection point of chord at toe in Table 6(a) is taken as an example and presented in Table 7. For a specific point of intersection, the fatigue damage factor S_a is first obtained and fixed according to equation (8). An initial SCF_{uni} value of 0.8 is randomly selected (with a reference to the values of $SCF_{equ(i)}$ in Table 7). The equivalent hot spot stresses for different wave directions are obtained respectively from equation (7), and subsequently the fatigue damage factor $S_e = 213.81$ is derived from equation (9). Since S_e is bigger than S_a, the value of SCF_{uni} is adjusted to a lower value of 0.6. Repeat the above steps (4)–(6) until S_e equals S_a, and the final SCF_{uni} value of 0.696 is determined for the intersection point of chord at toe as in Table 6(a). It is quite obvious that this iterative procedure is simple arithmetic and unconditionally stable. The convergence speed is very fast. Actually, the final SCF_{uni} can be obtained in just a few trial and error after obtaining the actual hot spot stress $\sigma_{ahot(i)}$ and the nominal stress $\sigma_{anom(i)}$ for short beam.

Following the same procedure, the unified SCFs for another selected joint at the lower guide of jack-up leg, as illustrated in Fig. 1, are also obtained. Table 8 compares the unified SCF values based on actual wave load cases with those based on basic load cases (see

Table 6
Unified SCFs for the selected joint at splash zone based on actual wave load cases.

i (deg)	Brace axial stresses F1	F2	F3	F4	$\sigma_{ahot(i)}$ (A)	$\sigma_{anom(i)}$ (B)	$SCF_{equ(i)}$ (= A/B)	$\sigma_{ehot(i)}$ (=B*C)	SCF_{uni} (C)
(a) For Chord @ Toe									
0	−0.06	1.21	0.48	−2.80	1.401	2.102	0.667	1.463	0.696
30	1.89	−2.34	−1.85	−1.51	3.015	3.054	0.987	2.126	0.696
60	0.55	0.35	−1.28	−2.35	2.715	3.296	0.824	2.295	0.696
90	4.59	2.12	−2.88	−1.80	1.494	4.255	0.351	2.962	0.696
120	−0.90	0.90	−1.76	0.19	1.905	1.431	1.332	0.996	0.696
150	−0.35	4.95	−2.39	−2.09	2.665	4.071	0.655	2.834	0.696
180	0.81	−4.11	−0.13	2.75	1.393	2.375	0.587	1.653	0.696
210	−1.10	1.83	1.36	0.07	1.714	1.302	1.317	0.906	0.696
240	0.65	0.15	0.00	0.55	0.775	0.499	1.554	0.347	0.696
270	−4.80	−2.10	2.41	1.72	0.992	3.754	0.264	2.614	0.696
300	0.33	−1.24	3.23	−0.67	2.797	2.334	1.198	1.625	0.696
330	−0.37	−5.54	3.79	1.56	3.124	4.866	0.642	3.388	0.696
$S_a = S_e$					140.90			140.90	**0.696**
(b) For Brace @ Toe									
0	−0.06	1.21	0.48	−2.80	3.231	2.102	1.537	3.017	1.436
30	1.89	−2.34	−1.85	−1.51	4.742	3.054	1.553	4.384	1.436
60	0.55	0.35	−1.28	−2.35	4.804	3.296	1.457	4.733	1.436
90	4.59	2.12	−2.88	−1.80	5.850	4.255	1.375	6.109	1.436
120	−0.90	0.90	−1.76	0.19	2.497	1.431	1.746	2.054	1.436
150	−0.35	4.95	−2.39	−2.09	5.642	4.071	1.386	5.846	1.436
180	0.81	−4.11	−0.13	2.75	3.472	2.375	1.462	3.410	1.436
210	−1.10	1.83	1.36	0.07	2.209	1.302	1.697	1.869	1.436
240	0.65	0.15	0.00	0.55	0.806	0.499	1.616	0.716	1.436
270	−4.80	−2.10	2.41	1.72	5.063	3.754	1.349	5.390	1.436
300	0.33	−1.24	3.23	−0.67	4.205	2.334	1.802	3.351	1.436
330	−0.37	−5.54	3.79	1.56	6.924	4.866	1.423	6.986	1.436
$S_a = S_e$					1235.84			1235.84	**1.436**
(c) For Chord @ Heel									
0	−0.06	1.21	0.48	−2.80	0.537	2.102	0.256	0.537	0.255
30	1.89	−2.34	−1.85	−1.51	0.862	3.054	0.282	0.780	0.255
60	0.55	0.35	−1.28	−2.35	0.673	3.296	0.204	0.842	0.255
90	4.59	2.12	−2.88	−1.80	1.205	4.255	0.283	1.086	0.255
120	−0.90	0.90	−1.76	0.19	0.469	1.431	0.328	0.365	0.255
150	−0.35	4.95	−2.39	−2.09	0.693	4.071	0.170	1.040	0.255
180	0.81	−4.11	−0.13	2.75	0.177	2.375	0.075	0.606	0.255
210	−1.10	1.83	1.36	0.07	0.401	1.302	0.308	0.332	0.255
240	0.65	0.15	0.00	0.55	0.385	0.499	0.772	0.127	0.255
270	−4.80	−2.10	2.41	1.72	1.322	3.754	0.352	0.959	0.255
300	0.33	−1.24	3.23	−0.67	0.731	2.334	0.313	0.596	0.255
330	−0.37	−5.54	3.79	1.56	0.943	4.866	0.194	1.242	0.255
$S_a = S_e$					6.95			6.95	**0.255**
(d) For Brace @ Heel									
0	−0.06	1.21	0.48	−2.80	0.905	2.102	0.431	1.751	0.833
30	1.89	−2.34	−1.85	−1.51	2.308	3.054	0.756	2.544	0.833
60	0.55	0.35	−1.28	−2.35	1.560	3.296	0.473	2.746	0.833
90	4.59	2.12	−2.88	−1.80	3.145	4.255	0.739	3.544	0.833
120	−0.90	0.90	−1.76	0.19	2.190	1.431	1.531	1.192	0.833
150	−0.35	4.95	−2.39	−2.09	2.622	4.071	0.644	3.392	0.833
180	0.81	−4.11	−0.13	2.75	0.605	2.375	0.255	1.979	0.833
210	−1.10	1.83	1.36	0.07	1.734	1.302	1.332	1.085	0.833
240	0.65	0.15	0.00	0.55	0.231	0.499	0.463	0.415	0.833
270	−4.80	−2.10	2.41	1.72	2.556	3.754	0.681	3.127	0.833
300	0.33	−1.24	3.23	−0.67	3.990	2.334	1.710	1.944	0.833
330	−0.37	−5.54	3.79	1.56	4.296	4.866	0.883	4.054	0.833
$S_a = S_e$					241.42			241.42	**0.833**

(*continued on next page*)

Table 6 (*continued*)

i (deg)	Brace axial stresses F1	F2	F3	F4	$\sigma_{ahot(i)}$ (A)	$\sigma_{anom(i)}$ (B)	$SCF_{equ(i)}$ (= A/B)	$\sigma_{ehot(i)}$ (=B*C)	SCF_{uni} (C)
(e) For Chord @ Saddle									
0	−0.06	1.21	0.48	−2.80	0.780	2.102	0.371	1.104	0.525
30	1.89	−2.34	−1.85	−1.51	0.700	3.054	0.229	1.604	0.525
60	0.55	0.35	−1.28	−2.35	0.521	3.296	0.158	1.731	0.525
90	4.59	2.12	−2.88	−1.80	1.397	4.255	0.328	2.234	0.525
120	−0.90	0.90	−1.76	0.19	1.574	1.431	1.100	0.751	0.525
150	−0.35	4.95	−2.39	−2.09	1.904	4.071	0.468	2.138	0.525
180	0.81	−4.11	−0.13	2.75	0.865	2.375	0.364	1.247	0.525
210	−1.10	1.83	1.36	0.07	0.724	1.302	0.556	0.684	0.525
240	0.65	0.15	0.00	0.55	0.160	0.499	0.321	0.262	0.525
270	−4.80	−2.10	2.41	1.72	1.092	3.754	0.291	1.971	0.525
300	0.33	−1.24	3.23	−0.67	2.636	2.334	1.129	1.226	0.525
330	−0.37	−5.54	3.79	1.56	2.937	4.866	0.604	2.555	0.525
$S_a = S_e$					60.47			60.47	**0.525**
(f) For Brace @ Saddle									
0	−0.06	1.21	0.48	−2.80	1.150	2.102	0.547	1.726	0.821
30	1.89	−2.34	−1.85	−1.51	1.732	3.054	0.567	2.508	0.821
60	0.55	0.35	−1.28	−2.35	1.095	3.296	0.332	2.708	0.821
90	4.59	2.12	−2.88	−1.80	2.600	4.255	0.611	3.495	0.821
120	−0.90	0.90	−1.76	0.19	2.380	1.431	1.664	1.175	0.821
150	−0.35	4.95	−2.39	−2.09	2.673	4.071	0.657	3.344	0.821
180	0.81	−4.11	−0.13	2.75	0.715	2.375	0.301	1.951	0.821
210	−1.10	1.83	1.36	0.07	1.512	1.302	1.161	1.069	0.821
240	0.65	0.15	0.00	0.55	0.109	0.499	0.219	0.410	0.821
270	−4.80	−2.10	2.41	1.72	2.001	3.754	0.533	3.084	0.821
300	0.33	−1.24	3.23	−0.67	4.221	2.334	1.809	1.917	0.821
330	−0.37	−5.54	3.79	1.56	4.417	4.866	0.908	3.997	0.821
$S_a = S_e$					231.40			231.40	**0.821**

Table 7
Detailed iteration process for calculating the unified SCF at the intersection point of chord @ toe in Table 6(a).

i (deg)	$\sigma_{ahot(i)}$ (A)	$\sigma_{anom(i)}$ (B)	$SCF_{equ(i)}$ (= A/B)	Iteration process for SCF_{uni}: SCF_{uni} (C)	$\sigma_{ehot(i)}$ (=B*C)	SCF_{uni} (C)	$\sigma_{ehot(i)}$ (=B*C)	SCF_{uni} (C)	$\sigma_{ehot(i)}$ (=B*C)	SCF_{uni} (C)	$\sigma_{ehot(i)}$ (=B*C)
0	1.401	2.102	0.667	0.800	1.682	0.600	1.261	0.700	1.471	0.696	1.463
30	3.015	3.054	0.987	0.800	2.443	0.600	1.832	0.700	2.138	0.696	2.126
60	2.715	3.296	0.824	0.800	2.637	0.600	1.978	0.700	2.307	0.696	2.295
90	1.494	4.255	0.351	0.800	3.404	0.600	2.553	0.700	2.979	0.696	2.962
120	1.905	1.431	1.332	0.800	1.145	0.600	0.859	0.700	1.002	0.696	0.996
150	2.665	4.071	0.655	0.800	3.257	0.600	2.443	0.700	2.850	0.696	2.834
180	1.393	2.375	0.587	0.800	1.900	0.600	1.425	0.700	1.663	0.696	1.653
210	1.714	1.302	1.317	0.800	1.042	0.600	0.781	0.700	0.911	0.696	0.906
240	0.775	0.499	1.554	0.800	0.399	0.600	0.299	0.700	0.349	0.696	0.347
270	0.992	3.754	0.264	0.800	3.003	0.600	2.252	0.700	2.628	0.696	2.614
300	2.797	2.334	1.198	0.800	1.867	0.600	1.400	0.700	1.634	0.696	1.625
330	3.124	4.866	0.642	0.800	3.893	0.600	2.920	0.700	3.406	0.696	3.388
S_a / S_e	**140.90**				213.81 ($S_e>S_a$)		90.21 ($S_e<S_a$)		143.25 ($S_e>S_a$)	**0.696**	**140.90** ($S_e=S_a$)

Column 1) as in Section 3.1. The percentage errors of the unified SCFs for the selected joints are listed in the last two columns. For the joint at the lower guide, the error percentage is generally less than 7.5%. For the joint at the splash zone, the error percentage is generally less than 12%. Due to the small SCF values, the percentage errors for the location of chord at heel are relatively large for both joints. Therefore, it can be concluded that the unified SCF values derived based on basic load cases are in good agreement with the joint SCFs at both splash zone and lower guide calculated based on actual wave loading. In other words, the unified SCFs calculated based on basic load cases can provide consistent fatigue damage with actual wave load cases.

The unified SCF values calculated based on all basic cases ($n = 9$ in equation (6)), including balanced, unbalanced and over-balanced loadings, are also presented in Table 8 (Column 2). It can be seen that there is no much difference between the SCF values at

Table 8
Comparison of the unified SCF values based on basic load cases and actual wave loading.

Location	Based on basic load cases		Based on actual wave loading			
	Balanced (A)	All axial (B)	Splash zone (C)	Lower guide (D)	Error percentage with Balanced	
					|C-A|/A×100%	|D-A|/A×100%
Chord @ Toe	0.632	0.796	0.696	0.645	10.1%	2.1%
Brace @ Toe	1.494	1.496	1.436	1.490	3.9%	0.3%
Chord @ Heel	0.159	0.341	0.255	0.212	60.4%	33.3%
Brace @ Heel	0.944	0.944	0.833	0.921	11.8%	2.4%
Chord @ Saddle	0.474	0.519	0.525	0.509	10.8%	7.4%
Brace @ Saddle	0.861	0.875	0.821	0.847	4.6%	1.6%

various intersections (toe, heel and saddle) on the brace side based on basic balanced load cases and those based on all axial load cases. However, with the introduction of unbalanced and over-balanced loadings, the SCFs at brace-to-chord intersections on the chord side based on all axial load cases have larger values than those just based on balanced loading. This is in line with the finding by Efthymiou and Durkin [4] that overlapping significantly reduces chord SCFs under balanced axial loading, which indirectly proves the validity of the proposed framework.

To illustrate the effects of using $m = 5$ in equation (6) and subsequent equations (8)–(9) on the calculation results of the unified SCF values based on basic load cases and actual wave loading, Table 9 lists the comparison of the unified SCF values for using $m = 3$ or 5 for the selected joint at splash zone. It can be found that the error percentages between the unified SCF values based on basic load cases and those based on actual wave loading for $m = 5$ are similar to those for $m = 3$. Therefore, it is demonstrated that the proposed framework of deriving the unified SCF is robust with reference to the inverse slope of the *S-N* curves at different scenarios.

Consequently, it is proposed in this paper that the unified SCFs for the short beam in the equivalent joint stick model can simply be derived from basic balanced load cases, instead of actual wave loading. That is, rather than using a detailed finite element model and tediously computing the SCF for the selected multi-planar overlapped joint as described in Section 2.2, a simple yet reliable joint stick model can be adopted to readily and accurately derive the unified SCF values only from basic balanced load cases (see Table 1). Therefore, in the context of offshore fatigue design and analysis, computational efficiency will be tremendously improved as it is very time-consuming to conduct FE analysis with a very fine mesh to get the SCFs for a number of multi-planar overlapped joint models located at different leg parts of jack-up. Alternatively, the multi-planar overlapped tubular joint may be implemented by taking into account the cross influencing effects as one super element [31] integrated with global beam model in an efficient and optimized manner.

3.3. The unified SCFs based on basic bending cases

As stated previously, the fatigue performance of jack-up leg joints mainly depends on the SCFs due to axial loading. The purpose of this section is just to extend the proposed framework to the bending conditions and provide a full image for the unified SCFs.

Table 10 shows the schematic view of both in-plane bending (IPB) and out-of-plane bending (OPB) cases for the overlapped joint. According to the procedure in Section 3.1, the equivalent SCFs for bending load cases are presented in Table 11. Unified SCF values for bending cases could be conservatively taken as the larger values in the reference plane and multi-plane cases, as seen in Table 11 (the bolded numbers).

4. Conclusions

This paper presents a novel framework for deriving the unified SCF values for multi-planar overlapped tubular *KK*-joint, which is commonly used in the leg structures of offshore jack-ups. Integrating the equivalent beam modeling with solid finite element model for the selected joints in the jack-up legs, the procedures for calculating the unified SCFs in the equivalent beam stick model are

Table 9
Comparison of the unified SCF values for using $m = 3$ or 5 for the selected joint at splash zone.

Location	$m = 3$			$m = 5$		
	Basic load cases	Actual wave loading	Error percentage	Basic load cases	Actual wave loading	Error percentage
Chord @ Toe	0.632	0.696	10.1%	0.637	0.689	8.2%
Brace @ Toe	1.494	1.436	3.9%	1.498	1.417	5.4%
Chord @ Heel	0.159	0.255	60.4%	0.169	0.262	55.0%
Brace @ Heel	0.944	0.833	11.8%	1.061	0.857	19.2%
Chord @ Saddle	0.474	0.525	10.8%	0.521	0.564	8.3%
Brace @ Saddle	0.861	0.821	4.6%	0.972	0.870	10.5%

Table 10
Schematic view of bending cases for the multi-planar overlapped *KK*-joint.

Load case	In-plane bending (IPB)	Out-of-plane bending (OPB)
Reference plane	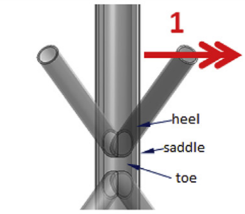	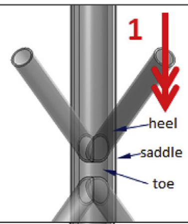
Multi-plane	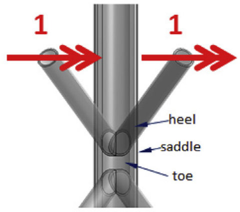	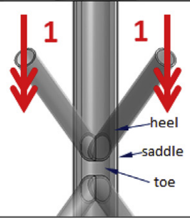

Table 11
Calculation of equivalent SCFs for bending load cases.

Load case (i)		IPB-Reference	IPB-Multi-plane	OPB-Reference	OPB-Multi-plane
$\sigma_{bhot(i)}$	Chord @ Toe	0.360	0.503	0.017	0.327
	Brace @ Toe	0.716	1.095	0.140	0.886
	Chord @ Heel	0.178	0.247	0.225	0.410
	Brace @ Heel	1.550	1.587	0.158	0.309
	Chord @ Saddle	0.000	0.000	0.515	0.621
	Brace @ Saddle	0.117	0.000	1.070	1.152
$\sigma_{bnor(i)}$	Short beam IPB	0.860	1.720	/	/
	Short beam OPB	/	/	0.950	1.900
$SCF_{equ(i)}$	Chord @ Toe	**0.419**	0.292	0.018	**0.172**
	Brace @ Toe	**0.833**	0.637	0.147	**0.466**
	Chord @ Heel	**0.207**	0.144	**0.237**	0.216
	Brace @ Heel	**1.802**	0.923	**0.166**	0.163
	Chord @ Saddle	**0.000**	0.000	**0.542**	0.327
	Brace @ Saddle	**0.136**	0.000	**1.126**	0.606

successfully developed based on basic load cases as well as actual wave load cases. The main findings from current studies are as follows:

(1) SCF of the multi-planar overlapped joint is often determined by finite element modeling. However, the computed SCF values might be not reliable in the context of fatigue design for offshore practical applications. Inspired by this, the unified SCF proposed in this paper is derived in relation to the fatigue damage.
(2) Following structural design of jack-up lattice leg, the out-of-plane overlapped *KK*-joint is mainly subject to axial loading. This constitutes the fundamental in deriving the unified SCF values based on basic axial load cases.

In view of the complexity of *KK*-joint, the proposed joint beam model reduces SCF modeling from multi-planar out-of-plane overlapping to equivalent uniplanar non-overlapping. The unified SCF values are obtained for the beam stick model based on basic load cases and verified by actual wave loading. Therefore, it is concluded that the unified SCFs for the equivalent joint beam model can be accurately derived just based on basic load cases. In the context of fatigue analysis, this will lead to huge saving in computational time as it is no need to use traditional FE techniques to evaluate the SCF values for the multi-planar overlapped joints encountered in offshore jack-up legs. As an alternative, super element techniques [31] may be considered as another efficient way by taking into account the multi-planar overlapped tubular joint as one super element in an integrated simulation model.

(3) Only out-of-plane overlapped *KK*-joint is studied here. Nevertheless, the proposed framework can be readily generalized to other kinds of overlapped joints, like *KK*-joint with in-plane overlapping and *KT*-joint in the lower guide of jack-up (see Fig. 1). For overlapped joint mainly subject to bending loads, the framework might be still applicable by considering the unified SCFs based on IPB and/or OPB load cases. This is recommended for further investigation.

Acknowledgements

This research is supported by the Research Start-up Foundation for Advanced Talent of Jiangsu University, Six Talent Peaks Project in Jiangsu Province (No. 2017-KTHY-010), and Major International Cooperation Project of National Natural Science Foundation of China (No. 11520101001). The authors would like to thank the Editor and the anonymous reviewers for their constructive comments and valuable suggestions to improve the quality of this article.

References

[1] Zhang J, Koh CG, Trinh TN, Wang XM, Zhang Z. Identification of jack-up spudcan fixity by an output-only substructural strategy. Mar Struct 2012;29:71–88.
[2] DNVGL-RP-C203. Fatigue Design of Offshore Steel Structures. DNV GL AS; April 2016.
[3] DNVGL-RP-C104. Self-Elevating Units. DNV GL AS; July 2015.
[4] Efthymiou M, Durkin S. Stress concentrations in T/Y and gap/overlap K-joints. Behav Offshore Struct 1985:429–40.
[5] Hellier AK, Connolly MP, Dover WD. Stress concentration factors for tubular Y- and T-joints. Int J Fatig 1990;12:13–23.
[6] Karamanos SA, Romeijn A, Wardenier J. Stress concentrations in tubular gap K-joints: mechanics and fatigue design. Eng Struct 2000;22:4–14.
[7] Myers PT, Brennan FP, Dover WD. The effect of rack/rib plate on the stress concentration factors in jack-up chords. Mar Struct 2001;14:485–505.
[8] Gao F, Shao YB, Gho WM. Stress and strain concentration factors of completely overlapped tubular joints under lap brace IPB load. J Constr Steel Res 2007;63:305–16.
[9] Yang J, Shao YB, Chen C. Static strength of chord reinforced tubular Y-joints under axial loading. Mar Struct 2012;29:226–45.
[10] Ahmadi H, Lotfollahi-Yaghin MA, Shao YB, Aminfar MH. Parametric study and formulation of outer-brace geometric stress concentration factors in internally ring-stiffened tubular KT-joints of offshore structures. Appl Ocean Res 2012;38:74–91.
[11] Shen W, Choo YS. Stress intensity factor for a tubular T-joint with grouted chord. Eng Struct 2012;35:37–47.
[12] Liu G, Zhao XL, Huang Y. Prediction of stress distribution along the intersection of tubular T-joints by a novel structural stress approach. Int J Fatig 2015;80:216–30.
[13] Karamanos SA, Romeijn A, Wardenier J. Stress concentrations in multi-planar welded CHS XX-connections. J Constr Steel Res 1999;50:259–82.
[14] Chiew SP, Soh CK, Wu NW. General SCF design equations for steel multiplanar tubular XX-joints. Int J Fatig 2000;22:283–93.
[15] Karamanos SA, Romeijn A, Wardenier J. Stress concentrations in tubular DT-joints for fatigue design. J Struct Eng 2000;126:1320–30.
[16] Karamanos SA, Romeijn A, Wardenier J. SCF equations in multi-planar welded tubular DT-joints including bending effects. Mar Struct 2002;15:157–73.
[17] van Wingerde AM, Packer JA, Wardenier J. Simplified SCF formulae and graphs for CHS and RHS K- and KK-connections. J Constr Steel Res 2001;57:221–52.
[18] Woghiren CO, Brennan FP. Weld toe stress concentrations in multi-planar stiffened tubular KK joints. Int J Fatig 2009;31:164–72.
[19] Lotfollahi-Yaghin MA, Ahmadi H. Geometric stress distribution along the weld toe of the outer brace in two-planar tubular DKT-joints: parametric study and deriving the SCF design equations. Mar Struct 2011;24:239–60.
[20] Ahmadi H, Zavvar E. The effect of multi-planarity on the SCFs in offshore tubular KT-joints subjected to in-plane and out-of-plane bending loads. Thin-Walled Struct 2016;106:148–65.
[21] Zhao XL, Herion S, Packer JA, Puthli R, Sedlacek G, Wardenier J, et al. Design guide for circular and rectangular hollow section welded joints under fatigue loading. CIDECT Publication, No. 8. Germany: TUV Verlag; 2000.
[22] Lee CK, Chiew SP, Lie ST, Sopha T, Nguyen TBN. Experimental studies on stress concentration factors for partially overlapped circular hollow section K-joints. Adv Steel Construct 2009;5:481–99.
[23] Bouwkamp JG. Concept of tubular-joint design. ASCE J Struct Div 1964;90.
[24] Tizani WMK, Yusurf KO, Davies G, Smith NJ. A knowledge based system to support joint fabrication decision making at the design stage – case study for CHS trusses. Proceedings of the 7th international symposium on tubular structures, Hungary. 1996. p. 483–9.
[25] Gibstein MB. Stress concentration in tubular K-joints with diameter ratio equal to one. Steel in marine structures. Amsterdam: Elsevier; 1987. p. 377–93.
[26] Dharmavasan S, Seneviratne LD. Stress analysis of POCHS K-joints, fatigue and crack growth in offshore structures. Inst Mech Eng 1986;2:17–30.
[27] Lee CK, Chiew SP, Lie ST, Sopha T. Comparison of fatigue performances of gapped and partially overlapped CHS K-joints. Eng Struct 2011;33:44–52.
[28] Gho WM, Gao F, Yang Y. Strain and stress concentration of completely overlapped tubular CHS joints under basic loadings. J Constr Steel Res 2006;62:656–74.
[29] Pang NL, Zhao XL, Mashiri FR, Dayawansa P. Full-size testing to determine stress concentration factors of dragline tubular joints. Eng Struct 2009;31:43–56.
[30] ANSYS. ANSYS Release 15.0 Documentation. 2013.
[31] Dubois J, Muskulus M, Schaumann P. Advanced representation of tubular joints in jacket model for offshore wind turbine simulation. Energy Proced 2013;35:234–43.